REPORT DOCUMENTATION PAGE

Form Approved
OMB NO. 0704-0188

1. AGENCY USE ONLY (Leave Blank)	2. REPORT DATE	3. REPORT TYPE AND DATES COVERED
	October, 2003	Final Technical Report ~~6/00-7/03~~ 19 Jun 00 - 18 Jun 03

4. TITLE AND SUBTITLE
Fabrication and Optical Recombination in III-Nitride Microstructures and Devices

5. FUNDING NUMBERS
DAAD19-00-1-0410

6. AUTHOR(S)
Hongxing Jiang and Jingyu Lin

7. PERFORMING ORGANIZATION NAME(S) AND ADDRESS(ES)
Kansas State University, Department of Physics, Manhattan, KS 66506-2601

8. PERFORMING ORGANIZATION REPORT NUMBER DAAD19-00-1-0410-(3)

9. SPONSORING / MONITORING AGENCY NAME(S) AND ADDRESS(ES)
U. S. Army Research Office
P.O. Box 12211
Research Triangle Park, NC 27709-2211

10. SPONSORING / MONITORING AGENCY REPORT NUMBER
~~Dr. John Zavada~~
40119.1-EL

11. SUPPLEMENTARY NOTES
The views, opinions and/or findings contained in this report are those of the author(s) and should not be construed as an official Department of the Army position, policy or decision, unless so designated by other documentation.

12 a. DISTRIBUTION / AVAILABILITY STATEMENT
Approved for public release; distribution unlimited.

12 b. DISTRIBUTION CODE

13. ABSTRACT (Maximum 200 words)

The research program at Kansas State University is to develop innovative approaches for fabricating high quality III-nitride QWs, heterostructures, microstructures, and micro-devices and to study their optical and optoeletronic properties. By optimizing the epilayer mobilities and optical emission properties, we have produced GaN, $Al_xGa_{1-x}N$ (x up to 1), $In_xGa_{1-x}N$ (x<0.3), and $In_xAl_yGa_{1-x-y}N$ epilayers, III-nitride QWs with device qualities. We have successfully fabricated micro-size blue emitters and developed a bonding scheme that allows us to address micro-size pixels individually in an array comprising many III-nitride micro-emitters/micro-detectors. We have demonstrated the operation of the first prototype blue microdisplay made from InGaN/GaN QWs. We have achieved highly conductive n-type $Al_xGa_{1-x}N$ alloys of high Al contents (for x up to 0.8). We have developed Mg-δ-doping for enhanced p-type doping efficiency in GaN and AlGaN. A 2-fold enhancement in lateral and a 5-fold enhancement in vertical p-type conductions have been achieved for GaN and AlGaN epilayers. We have also achieved AlN epilayers with very efficient *band-edge* PL emission — the optical quality of AlN is comparable to that of GaN and determined the detailed band structure near the Γ-point of wurtzite AlN, including energy gap, optical selection rules, exciton binding energies and lifetimes, and acceptor/donor energy levels.

14. SUBJECT TERMS	15. NUMBER OF PAGES
III-nitride wide band gap semiconductors, micro-size light emitters, optical and optoelectronic properties, nano-technologies	15
	16. PRICE CODE

17. SECURITY CLASSIFICATION OR REPORT	18. SECURITY CLASSIFICATION ON THIS PAGE	19. SECURITY CLASSIFICATION OF ABSTRACT	20. LIMITATION OF ABSTRACT
UNCLASSIFIED	**UNCLASSIFIED**	**UNCLASSIFIED**	**UL**

NSN 7540-01-280-5500

Standard Form 298 (Rev.2-89)
Prescribed by ANSI Std. 239-18
298-102

REPORT DOCUMENTATION PAGE (SF298)
(Continuation Sheet)

Final Technical Report

Award No: DAAD19-00-1-0410
Period Covered: 06/2000 – 07/2003
Project Title: Fabrication and Optical Recombination in III-Nitride Microstructures and Devices
PI Name: Hongxing Jiang & Jingyu Lin
PI Address: Department of Physics, Kansas State University, Manhattan, KS 66506-2601
Tel: (785)532-1627, Fax: (785)532-5636, e-mail: jiang@phys.ksu.edu
Tel: (785)532-1616, Fax: (785)532-5636, e-mail: jylin@phys.ksu.edu

I. Brief Summary of Progress

The research program at Kansas State University is to develop innovative approaches for fabricating high quality III-nitride QWs, heterostructures, microstructures, and micro-devices and to study their optical and optoeletronic properties. By optimizing the epilayer mobilities and optical emission properties, we have produced GaN, $Al_xGa_{1-x}N$ (x up to 1), $In_xGa_{1-x}N$ (x<0.3), and $In_xAl_yGa_{1-x-y}N$ epilayers, III-nitride QWs with device qualities. Most recently, we have successfully fabricated micro-size blue emitters. We have also developed a bonding scheme that allows us to address micro-size pixels individually in an array comprising many III-nitride micro-emitters/micro-detectors. For examples, when an array of microdisks was forward biased and individually addressed, we have successfully demonstrated the operation of the World's first prototype blue microdisplay made from InGaN/GaN QWs. The bonding scheme of these microdisplays can also be utilized to study fundamental properties of individual III-nitride micro-size light emitters under current injection conditions, which is important for developing the knowledge base for future III-nitride micron and nano-size optoelectronic devices. Within the funding period, we have achieved highly conductive n-type $Al_xGa_{1-x}N$ alloys of high Al contents (for x up to 0.8). We have developed Mg-δ-doping for enhanced p-type doping efficiency in GaN and AlGaN. A 2-fold enhancement in lateral and a 5-fold enhancement in vertical p-type conductions have been achieved for GaN and AlGaN epilayers. We have also achieved AlN epilayers with very efficient *band-edge* PL emission — the optical quality of AlN is comparable to that of GaN and determined the detailed band structure near the Γ-point of wurtzite AlN, including energy gap, optical selection rules, exciton binding energies and lifetimes, and acceptor/donor energy levels.

Here we give a few examples of our accomplishments during the period of support. More details can be found in the publications listed in our group's web-site: http://www.phys.ksu.edu/area/GaNgroup, and a partial list is provided in section II.

i. Optimizing MOCVD growth technologies

During the funding period, our group has developed comprehensive techniques for MOCVD growth of III-nitride materials. By optimizing the epilayer mobilities and optical emission properties, we have produced GaN, $Al_xGa_{1-x}N$ (x up 1), $In_xGa_{1-x}N$ (x<0.7), and $In_xAl_yGa_{1-x-y}N$ (y<0.2) epilayers, InGaN/GaN, GaN/AlGaN, AlGaN/AlN and $In_xAl_yGa_{1-x-y}N$/GaN QWs/heterojunctions with device qualities. Currently, our undoped n-type GaN epilayers exhibit room temperature background electron concentration around 5×10^{16} cm^{-3} and mobility 650 cm^2/Vs. We have achieved p-type GaN with free hole concentration as high as $2 \times 10^{18} cm^{-3}$ [e.g., see Fig. 10] and mobility around 10 cm^2/Vs. For the first time, we have achieved highly conductive n-type $Al_xGa_{1-x}N$ with high Al contents (x up to 0.7) and p-type $Al_xGa_{1-x}N$ for x up to 0.27. The power output for our purple (408 nm) and blue (460 nm) light emitting diodes (LEDs) is about 3.0 mW at 20 mA.

ii. Growth and optical studies of high quality GaN/AlGaN Multiple Quantum Wells

$GaN/Al_xGa_{1-x}N$ and $In_xGa_{1-x}N/GaN$ MQWs with varying structural parameters have been grown by our MOCVD system. The optimized $GaN/Al_xGa_{1-x}N$ MQW structures exhibited extremely high quantum efficiencies as well as a ratio of well to barrier emission intensity exceeding 10^4. This is highly preferred for laser and LED applications, since one important issue in the laser and LED structure design is to maximize the optical emission or quantum efficiency in the well regions [Figs. 1 & 2].

The AlN/GaN heterostructures is the first semiconductor system that offers an energy band gap difference between the barrier and well materials as large as 2.8 eV. However, very little work has been done so far for AlN/GaN heterostructures and QWs. Most recently, we have investigated the growth of GaN/AlN and AlGaN/AlN heterostructures and MQWs. We have employed deep UV (λ down to 200 nm) picosecond time-resolved PL measurements to probe the optical quality of these structures. When the growth conditions of AlN/GaN MQWs were optimized, for the first time, we observed the interband transitions of the ground and the first excited states, [n=1e $\rightarrow$ n=1h] and [n=2e $\rightarrow$ n=2h] in the wells at 4.039 and 5.371 eV, respectively. The recombination lifetimes of these two interband transitions have been measured.

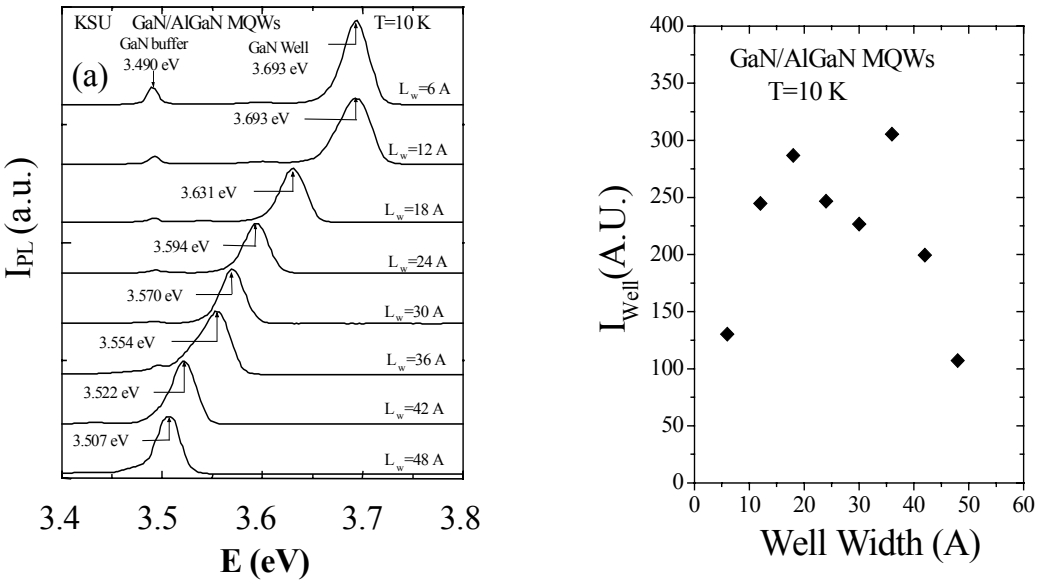

Fig. 1 (a) PL emission spectra of our GaN/AlGaN MQWs with varying well widths, L_W, but a fixed barrier width of 50 Å. The main emission lines are blue shifted with respect to the GaN epilayer, due to the effect of quantum confinement. The spectral peak position shift with L_W directly reflects the effects of the piezoelectric and polarization fields as well as the effect of quantum confinement in GaN/AlGaN MQWs. The observed spectral linewidths are among those narrowest ones reported. (b) The integrated well emission intensity versus well width for the $GaN/Al_xGa_{1-x}N$ MQWs measured at 10 K, which shows that highest quantum efficiencies are achieved when the well width is between 12 and 42 Å.

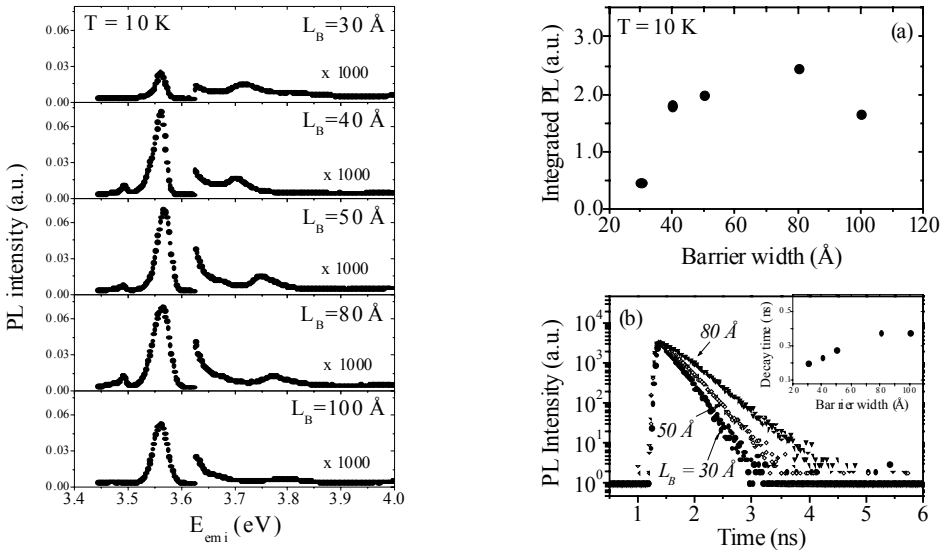

Fig. 2 (Left) PL spectra of a set of 30 Å well GaN/$Al_xGa_{1-x}N$ MQW samples with varying barrier widths, L_B = 30, 40 50, 80, and 100 Å, measured at 10 K. The MQW structures are grown under identical conditions. A ratio of well emission intensity to barrier emission intensity exceeding 10^4 has been achieved. (Right *a*) Integrated PL intensity of the well transition for the GaN/$Al_xGa_{1-x}N$ MQW samples as a function of the barrier width measured at 10 K. (Right b) The temporal responses of the well transitions in the GaN/$Al_xGa_{1-x}N$ MQW samples for various barrier widths at 10 K. The PL decay in all MQW samples studied here can be well described by a single exponential decay function. The inset shows the barrier width dependence of the decay lifetime for the well transition. Our studies here have shown that the optimal GaN/AlGaN ($x \sim 0.2$) MQW structures for UV light emitter applications are those with barrier widths ranging from 40 to 80 Å.

2. Growth and optoelectronic properties of III-nitride quaternary alloys

$In_xAl_yGa_{1-x}N$ quaternary alloys with different In and Al compositions were grown on sapphire substrates with GaN buffer by metal-organic chemical vapor deposition (MOCVD). Optical properties of these quaternary alloys were studied by picosecond time-resolved photoluminescence. Our studies have revealed that $In_xAl_yGa_{1-x}N$ quaternary alloys with lattice matched with GaN (y~4.7x) have the highest optical quality. More importantly, As shown in Fig. 3, we can achieve not only higher emission energies but also higher emission intensities (or quantum efficiencies) in $In_xAl_yGa_{1-x-y}N$ quaternary alloys than that of GaN. The quantum efficiency of $In_xAl_yGa_{1-x}N$ quaternary alloys was also enhanced significantly over AlGaN alloys with a comparable Al content. We have also fabricated ultraviolet (UV) photoconductive detectors based on $In_xAl_yGa_{1-x-y}N$/GaN quaternary alloy heterostructures. We found that with varying In and Al compositions, the cut-off wavelength of the $In_xAl_yGa_{1-x-y}N$ detectors could be varied to the deep UV range and that the responsivity of the $In_xAl_yGa_{1-x-y}N$ quaternary alloys exceeded that of AlGaN alloys with comparable cut-off wavelengths by a factor of five. This showed that $In_xAl_yGa_{1-x-y}N$ quaternary alloys is a very important material for solar-blind UV detector applications particularly in the deep UV range where Al rich AlGaN alloys have problems with low quantum efficiency and cracks due in part to lattice mismatch with GaN. Our results strongly suggested that $In_xAl_yGa_{1-x-y}N$ quaternary alloys open a new avenue for the fabrication of many novel optoelectronic devices such as high efficient light emitters and detectors, particularly in the UV region.

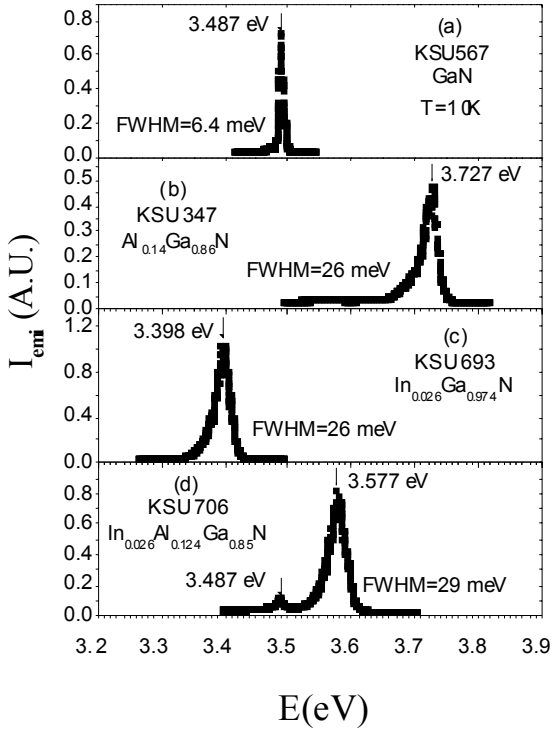

Fig. 3 PL emission spectra of GaN, AlGaN, InGaN, and InAlGaN epilayers grown by our MOCVD system. The emission spectrum of InAlGaN shows that we can achieve not only higher emission energies but also higher emission efficiency in the InAlGaN quaternary epilayers than that of GaN. The emission efficiency of the InAlGaN epilayers is also higher than that of the AlGaN epilayer and is comparable to that of the InGaN epilayer. These materials open a new avenue for the fabrication of high efficient light emitters and detectors operating in the UV region.

3. *Fabrication and optical investigations of III-nitride microstructures*

Our group has pioneered the fabrication of micro- and nano-size photonic structures and devices based on GaN wide bandgap semiconductors by e-beam and photo-lithographic patterning and plasma etching as well as by selective-area growth. An approximate 10-fold increase in quantum efficiency of the intrinsic transition upon formation of microstructures was observed in III-nitrides. We have fabricated and determined different optical resonance modes in the novel GaN pyramidal microcavities and showed that each pyramidal microcavity is a true 3D cavity that can support more than three different groups of optical resonance modes. Our work in this area has been featured in several popular national and international magazines including *Laser Focus World, III-Vs Review*, and *The Japanese Annual Report on Optoelectronic Industrial and Technical Trend Research.*

Recently our research group at Kansas State University has successfully fabricated electrically-pumped individual III-nitride micro-size LEDs and micro-LED arrays and observed enhanced quantum efficiencies. The micro-size LEDs were fabricated from our research laboratory grown LED wafers based on the InGaN/GaN QW LED structure. Our LED structures were grown on sapphire substrates with 30 nm GaN buffer layers. The QW device layers comprise 3.5 μm of Si-doped GaN, 0.1μm of silicon doped superlattice consisting alternating layers of 50 Å/50 Å of AlGaN/GaN, a 50 Å of silicon doped GaN, 20 Å undoped InGaN active layer, 0.14 μm of Mg doped superlattice consisting alternating layers of 50 Å /50 Å of AlGaN/GaN, and 0.5 μm Mg-doped GaN epilayer, followed by a rapid thermal anneal at 950 ^{o}C for 5 seconds in nitrogen. This process produced p-layer concentrations of $5x10^{17}$ (hole mobility 12 cm^2/Vs) and n-layer concentrations of $1.6x10^{18}$ (electron mobility 310 cm^2/Vs). By incorporating the AlGaN/GaN superlattice structure into our LED device layers, the p-type concentration was enhanced from 2 $x10^{17}$ to 5 x $10^{17}cm^{-3}$. Microdisk arrays such as that shown in Fig. 4 with individual disk size varying from 5 to 20 μm were fabricated by photolithographic patterning and inductively coupled plasma (ICP) dry etching. Bilayers of Ni (20nm)/Au (200nm) and Al (300nm)/Ti (20nm) were deposited by electron beam

evaporation as p- and n-type Ohmic contacts. The p- and n-type contacts were thermally annealed in nitrogen ambient for 5 min at 500 ^{0}C and 650 ^{0}C, respectively. The emission wavelengths of our micro-size LEDs vary from green to purple (390 to 450 nm) by varying In content in the InGaN active layers.

Fig. 4 Micro-size emitters based on InGaN/GaN QWs

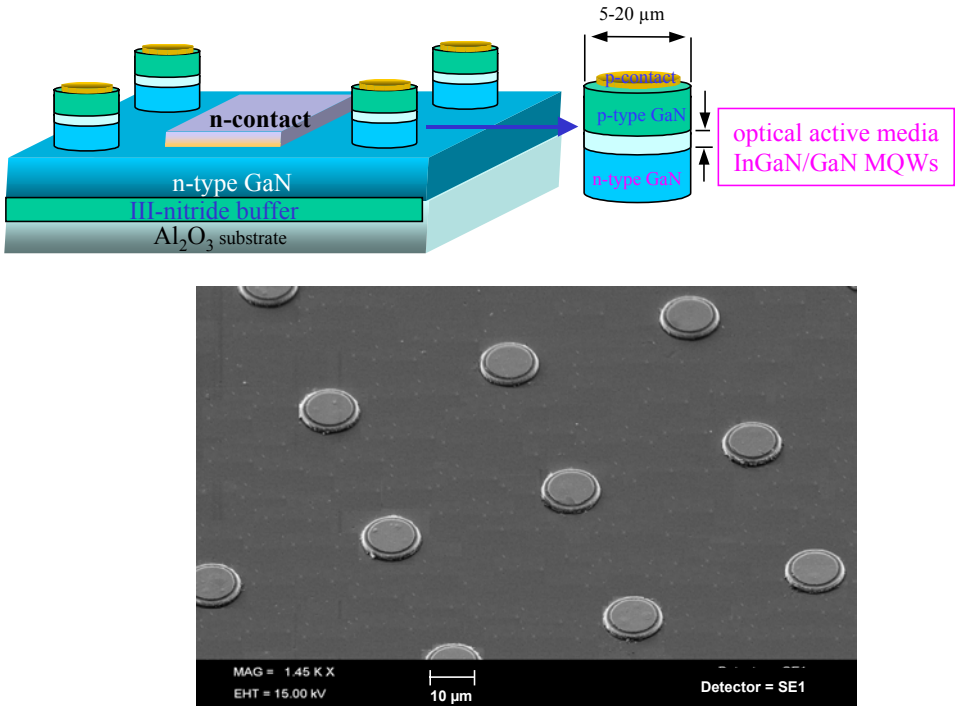

4. *Fabrication of integrated micro-size emitters for boosting emission efficiencies*

We have succeeded in interconnecting hundreds of III-nitride micro-size LEDs (size on the order of 10 μm in diameter). As illustrated in Fig. 5, these microdisk LEDs are interconnected in a manner that they are turned on and off simultaneously and fit into the same device area taken up by a conventional LED of about 300 x 300 μm^2. The performance characteristics of the novel devices were compared with those of the conventional LEDs fabricated from the same LED wafers. It was shown that, while the forward biased voltage (V_F) was slightly higher at 20 mA, the interconnected microdisk LEDs can boost the overall emission efficiency by 60%. It is believed that the novel device can overcome two biggest problems facing LEDs - the low extraction efficiencies due to the total internal reflection occurring at the LED/air interface and the problem of current spreading. Additionally, the strain induced piezoelectric field in the active QW regions may be reduced in micro-size LEDs, resulting in an increased internal quantum efficiency. Furthermore, the processing steps of these interconnected micro-size LEDs are the same as those of the conventional LEDs. It is thus expected the manufacture yield of these novel LEDs to rival with the conventional LEDs.

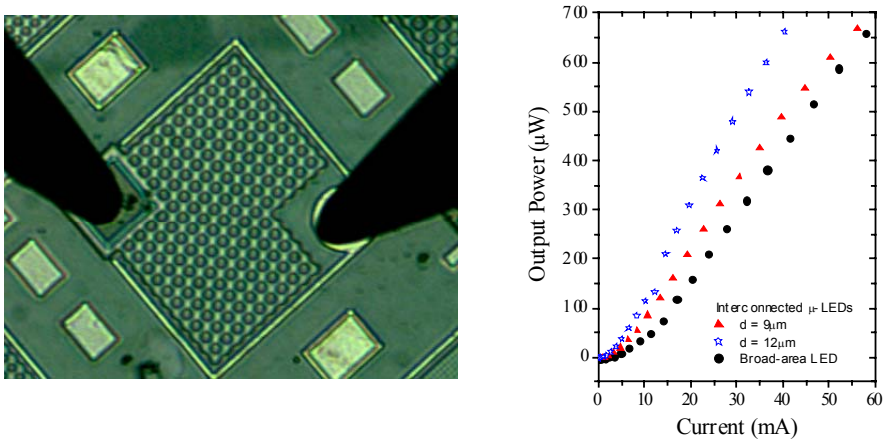

Fig. 5 We have succeeded in interconnecting together hundreds of microdisk LEDs (disk size on the order of 10 μm in diameter) made from InGaN/GaN single quantum wells grown by MOCVD. These interconnected microdisk LEDs fit into the same device area taken up by a conventional broad-area LED and boost LED emission efficiencies by 60%. It is believed that the novel device can overcome two biggest problems facing LEDs - the low extraction efficiencies due to the total internal reflection occurring at the LED/air interface and the problem of current spreading. (Left) Optical microscope image of a KSU interconnected μ-disk LEDs. (Right) Comparison of L-I characteristics of two interconnected InGaN/GaN QW μ-disk LEDs with individual disk diameter of 9 and 12 μm and a conventional broad-area LED fabricated from the same wafer measured on the top surface of unpackaged chips. Emission efficiency boosted by 60% in interconnected μ-disk LEDs. *This work was featured in Laser Focus World (Dec. 2000), Photonics Spectra (Dec. 2000), Compound Semiconductor (made the cover page of the Nov. 2000 issue).*

Our work on interconnected μ-disk LEDs has stimulated great interest in the optoelectronic device community and was featured in several popular magazines, including *Compound Semiconductor (made the cover of the Nov. 2000 issue), Laser Focus World (Dec. 2000 issue), and Photonics Spectra (Dec. 2000 issue)*. In this proposed research, we will explore methods to further enhance the LED emission efficiencies.

5. *Fabrication of III-Nitride Microdisplays*

We have also developed and patented a bonding scheme that allows us to address microcavity pixels individually in an array comprising many III-nitride micro-emitters/micro-detectors. For examples, when an array such as that of Fig. 4 was forward biased and individually addressed, we have successfully demonstrated the operation of a prototype blue microdisplay. The prototype device has a dimension of 0.5 x 0.5 mm^2 and consists of 10 x 10 pixels of 12 microns in diameter [Fig. 6(a)]. Figure 6(b) shows optical microscope images of a blue microdisplay in action, displaying letters USA. This demonstrates the operation of the first prototype semiconductor microdisplay.

Current microdisplays are based on liquid crystal display technology or organic light emitting diodes. High-information content semiconductor microdisplays, which require the integration of a dense array of micro-size LEDs on a single semiconductor chip, have not been successfully fabricated. Furthermore, color conversion for full color displays cannot be achieved in conventional III-V or Si semiconductors. So far, large flat panel displays based on semiconductor LEDs used on large buildings and stadiums are made up of a massive number of discrete LEDs. Based on the

results obtained from this prototype microdisplay and the unique properties of III-nitrides, we believe that III-nitride microdisplays can potentially provide unsurpassed performance including: self-luminescent, high brightness/resolution/contrast, high temperature/high power operation, high shock resistance, wide field-of-view, full color spectrum capability, long life, high speed, and low power consumption. On the other hand, the ability of 2D array integration with advantages of high speed, high resolution, low temperature sensitivity, and applicability under versatile conditions make III-nitride micro-LEDs as a potential candidate for light sources in short distance optical communications. Our III-nitride blue microdisplay work is to be featured in many popular magazines including *Laser Focus World*, *Photonics Spectra*, *Compound Semiconductor*, *III-Vs Review*, *Technology & Research News*, *Opto & Laser Europe*, etc.

The bonding scheme of these microdisplays was also utilized to characterize individual III-nitride micro-LEDs under current injection conditions.

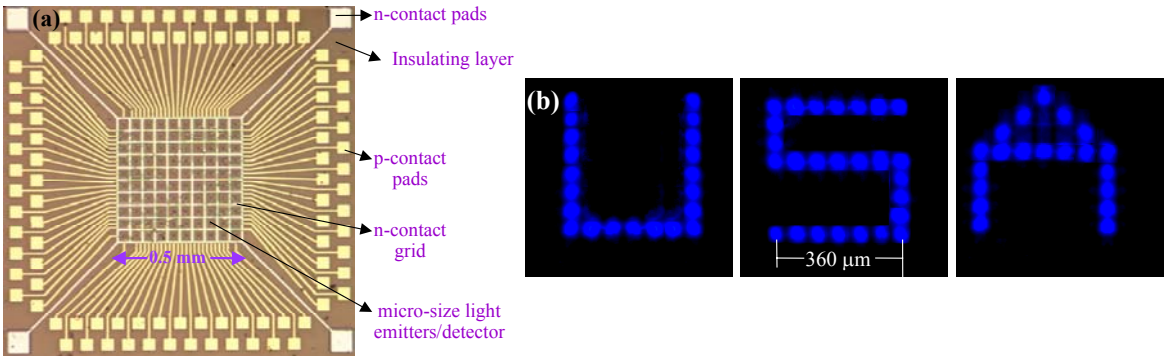

Figure 6 (a) Optical microscope image of a bonding scheme that allows us to address each microdisk pixel individually (or a III-nitride blue microdisplay); (b) Optical microscope image of the III-nitride blue microdisplay (a) in action, displaying letters "USA." [Work to be featured in many popular magazines including *Laser Focus World*, *Photonics Spectra*, *Compound Semiconductor*, *III-Vs Review*, *Technology & Research News*, *Opto & Laser Europe*, etc.]

6. Achieving p-type conduction in AlGaN alloys

During the funding period, we have achieved for the first time p-type conduction in AlGaN alloys (1 micron thick films) for AlN fraction up to 27%. Before this, p-type conduction was only demonstrated in AlGaN epilayers for AlN fraction up to 15%. A hole concentration of about 7 x 10^{16} cm^{-3} and mobility 3 cm^2/Vs at room temperature have been achieved in Mg-doped $Al_{0.27}Ga_{0.73}N$ epilayers, as confirmed by Hall measurements. The thermal activation energy (E_A) of Mg in $Al_xGa_{1-x}N$ as a function of x has been measured and is 0.31 eV at x=0.27.

The Mg-doped p-type $Al_xGa_{1-x}N$ epitaxial layers of thickness 1 μm were grown on sapphire substrates with a 30 nm GaN buffer layers. For Mg-doping, bis-cyclopentadienyl-magnesium (Cp_2Mg) was transported into the growth chamber with ammonia during growth. Postgrowth annealing at 950 ^oC in nitrogen gas ambient for 8 sec resulted in p-type conduction, as verified by Hall measurements. After a further anneal at 600 ^oC for 2 min in nitrogen gas, the recombination of free electrons with neutral Mg acceptor was observed to be the dominant emission lines at room temperature in $Al_xGa_{1-x}N$. The emission peaks were observed at 3.615 eV, 3.667 eV and 3.682 eV for x = 0.22, 0.25 and 0.27 respectively, from which the activation energy $E_A(x)$ of the ionized Mg

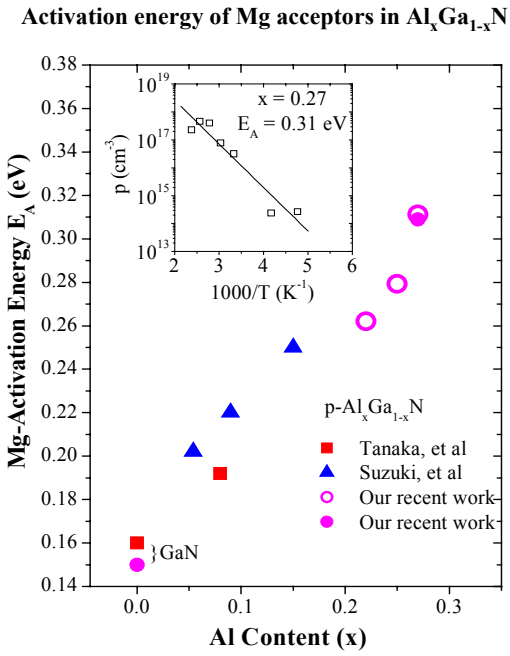

Fig. 7 Activation energy of Mg acceptors in Mg-doped p-type $Al_XGa_{1-X}N$ as a function of Al content x. Closed squares and triangles are data from refs. 25 and 26 respectively, while closed circles are data from our work. The inset shows the measured temperature dependence of the free hole concentration (p) in Mg-doped p-type $Al_{0.27}Ga_{0.73}N$ sample from which E_A = 0.310 eV was obtained.

impurity in $Al_xGa_{1-x}N$ can be deduced simply by the difference between the energy gap E_g (x) and the observed band-to-impurity emission peak $E(e^-,A^o)$. E_g (x) can be estimated from the expression

$$E_g(x) = (1-x)E_{g,GaN} + xE_{g,AlN} - bx(1-x) \qquad (1)$$

and $E_A(x) = E_g(x) - E(e^-,A^o)$. In the above expression, we use widely accepted value of the energy gap for GaN, $E_{g,GaN}$ = 3.42 eV, for AlN, $E_{g,AlN}$ = 6.20 eV and of the bowing parameter b = 0.90. With these, E_A values of 0.262 eV, 0.279 eV and 0.311 eV corresponding to Al contents 0.22, 0.25 and 0.27, respectively, are obtained. It is expected that different choices of the bowing parameter b would result in variations in the E_A values. However, because the Mg acceptor level in AlGaN alloys is quite deep, the uncertainties in E_A values due to different choices of b are not very significant. For example, the above optically determined E_A values from Eq. (1) will be reduced by about 17 - 20 meV if the bowing parameter b = 1 is used. The value of E_A we obtained in the above manner are plotted as a function of Al content x in Fig. 7, together with those reported previously, all obtained by means of variable temperature Hall measurements.

Also shown in this figure are data points for p-GaN and for p-$Al_{0.27}Ga_{0.73}N$ where we determined E_A by variable temperature Hall measurements (0.15 eV and 0.309 eV respectively). The measured temperature dependence of Hall concentration (p) in the Mg-doped p-type $Al_{0.27}Ga_{0.73}N$ sample is shown in the inset of Fig. 7, from which a value E_A = 0.310 eV was obtained. Since the hole concentrations in AlGaN alloys are relatively low and impurity band formation is not likely, our results of E_A deduced from the PL spectra match quite well with those obtained by Hall measurements. The results shown in the inset of Fig. 7 demonstrated conclusively that we have obtained p-type $Al_xGa_{1-x}N$ epilayers with x up to 0.27. A hole concentration of about 7 x 10^{16} cm^{-3} and mobility 3 cm^2/Vs at room temperature have been achieved in Mg-doped $Al_{0.27}Ga_{0.73}N$ epilayers.

The increase of E_A with increase in band gap energy for the III-nitrides has been reported previously in other studies and is predicted by the effective mass theory. As a comparison with our

results, the value of E_A estimated from the effective mass theory for x = 0.25 for example, is between 0.263 and 0.294 eV which agrees well with the measured value of 0.279 eV. From the measured E_A versus x in Mg-doped p-type $Al_xGa_{1-x}N$, the resistivity versus x can be estimated as follows:

$$\rho(Al_xGa_{1-x}N) = \rho_o exp(E_A/kT) = \rho_o exp\{[E_A(GaN) + \Delta E_A]/kT\} = \rho(GaN)\{exp(\Delta E_A]/kT)\} \quad (2)$$

where $\Delta E_A = E_A(Al_xGa_{1-x}N) - E_A(GaN)$ and our p-type GaN has typical resistivity, ρ(GaN), of about 1.0 Ω-cm. From Eq. (2), the resistivity of $Al_xGa_{1-x}N$ alloys with higher values of x can be deduced. For example, if the trend in Fig. 6 holds for higher x, at Al content x = 0.45, the activation energy E_A is estimated to be 0.4 eV and the estimated resistivity should be as high as 2.2 x 10^4 Ω-cm. This deepening of the Mg activation energy with Al content presents a real challenge for obtaining p-type AlGaN with high Al contents.

7. Delta-doping for Enhanced P-type Conduction in GaN and $Al_xGa_{1-x}N$ Alloys

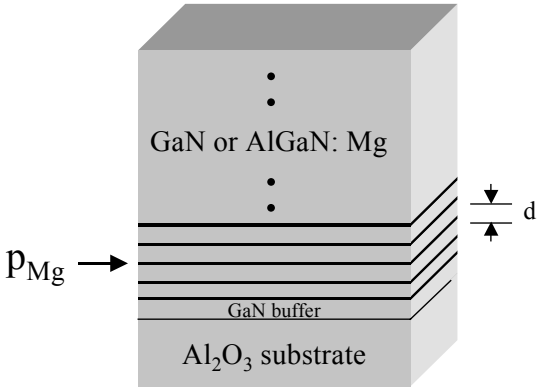

Fig. 8 Schematic diagram of Mg δ-doped GaN or AlGaN, where d (=15 nm) and P_{Mg} denote, respectively, the distance between two δ-planes and the two dimensional (2D) Mg doping concentration.

MOCVD allows the growth of mono-atomic layers, which makes the impurity doping within a single atomic layer (δ-doping) possible. Fig. 8 is a schematic diagram of Mg-δ-doped GaN or AlGaN epilayer. A δ-junction-like doping profile is implemented by interrupting the usual crystal-growth mode by closing the Ga (and Al) flow and leaving the N (NH_3) flow continuously. The N-stabilized crystal surface is thus maintained while the Mg impurities are introduced into the growth chamber so that an impurity-growth mode results. In this mode the host crystal does not continue to grow. It is hoped that by using this technique, a small fraction of available Ga sites in the δ-doped plane, typically $^1/_{10}$ to $^1/_{10000}$, will be occupied by Mg impurities. Recently, by employing Si-δ-doping in the barrier region of AlGaN/GaN heterojunction field effect transistor (HFET) structures, we have observed improved DC performances, i.e., enhanced maximum current, reduced leakage current, and increased breakdown voltage in Si-δ-doped structures over those of uniformly doped ones. We have carried out investigations in Mg-δ-doping in GaN and AlGaN and obtained extremely promising results. We have observed that δ-doping significantly suppresses the dislocation density in GaN and AlGaN epilayers. This is illustrated in Fig. 9, where AFM and SEM morphologies of etched layers of Mg-δ-doped and uniformly Mg-doped $Al_{0.07}Ga_{0.93}N$ epilayers are shown. The results demonstrate significant reduction of dislocation density (or etch pit density) in δ-doped p-type $Al_{0.07}Ga_{0.93}N$. The AFM images shown in Fig. 9 indicate that the etch pit density decreased by almost one order of magnitude from 7.9 x 10^7 cm^{-2} in uniformly Mg-doped layer to 0.9 x 10^7 cm^{-2} in Mg-δ-doped layer. The SEM images in Fig. 8 reveal a reduction of etch pit density from 9.4 x 10^7 cm^{-2} in uniformly Mg-doped p-type $Al_{0.07}Ga_{0.93}N$ layer to 1.8 x 10^7 cm^{-2} in Mg-δ-doped p-type $Al_{0.07}Ga_{0.93}N$ layer. The results thus strongly suggest that δ-doping can reduce dislocation density and hence improve the

overall material quality of III-nitrides in general, which will be extremely beneficial to the fabrication of optoelectronics and photonics devices, especially UV emitters. We believe that the observed reduction in dislocation density is due to the growth interruption in the Mg-δ-doping duration. Ga or Al atoms are halted during δ-doping, which stops the growth of GaN or AlGaN. It is known that growth interruption generally reduces the dislocation densities due to the partial termination of dislocation propagation in the growth direction.

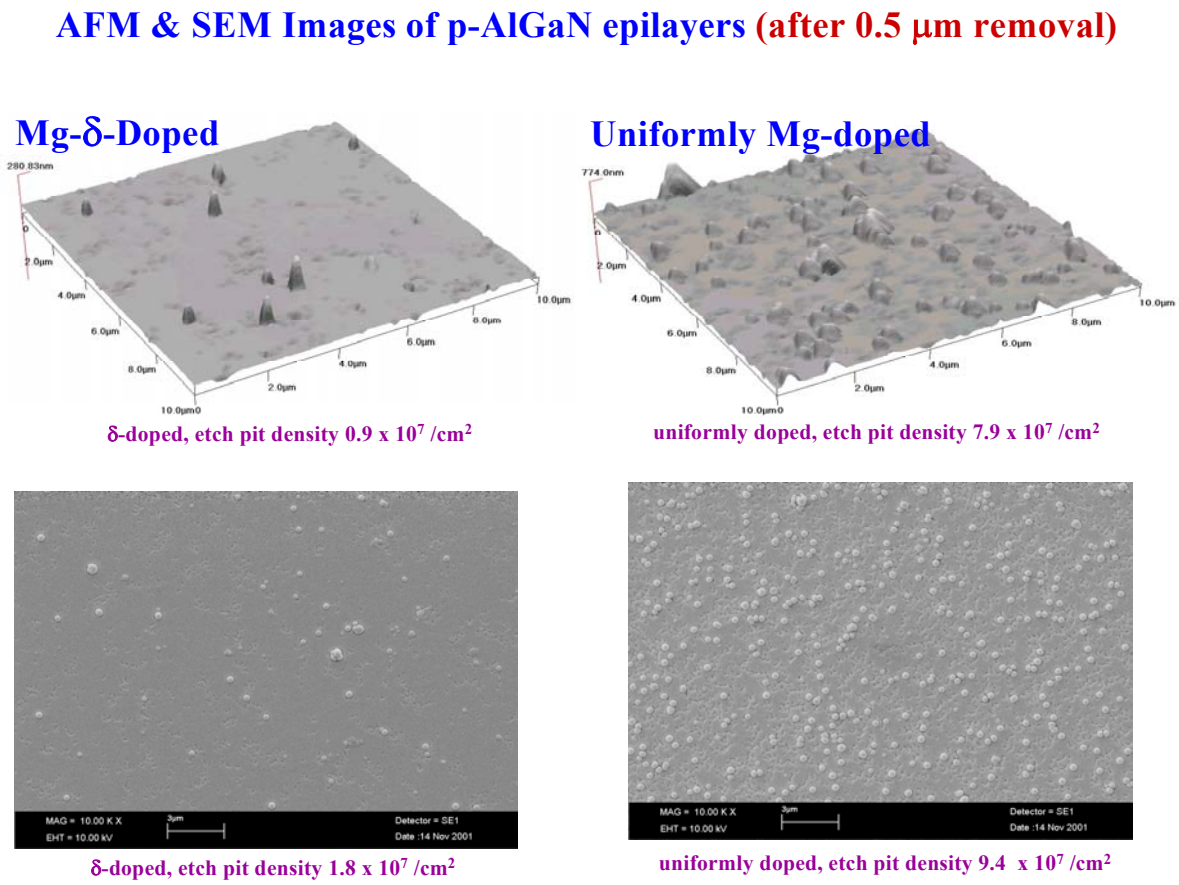

Fig. 9 AFM and SEM morphologies of etched surfaces of p-type AlGaN epilayers after a 0.5 μm removal by inductive-coupled plasma (ICP) etching. AFM images of (a) Mg-δ-doped and (b) uniformly Mg-doped p-type AlGaN epilayers. SEM images of (c) Mg-δ-doped and (d) uniformly Mg-doped p-type AlGaN epilayers. AFM and SEM images reveal that the etch pit density was significantly reduced in Mg-δ-doped p-type AlGaN compared with uniformly Mg-doped p-type AlGaN, implying a reduction of the dislocation density in Mg-δ-doped p-type AlGaN.

Additionally, Mg-δ-doped GaN and AlGaN epilayers exhibit much improved electrical properties over uniformly doped layers. For GaN, we have achieved a room temperature p-type resistivity of Mg-δ-doped p-GaN epilayers as low as 0.6 Ωcm (free hole concentration around 2 x 10^{18} cm^{-3} and mobility around 5 cm^2/Vs), while uniformly Mg-doped GaN epilayers typically exhibit a p-type resistivity greater than 1 Ωcm. It was observed that the Mg-δ-doping enhances only the hole concentration and induces no changes in the hole mobility. Similar results have been obtained for p-type AlGaN alloys. We plot the comparison results of the temperature dependent resistivity of uniformly Mg-doped and Mg-δ-doped p-type $Al_{0.07}Ga_{0.93}N$ epilayers in Fig. 10(a), which demonstrates a 2-fold reduction of resistivity at room temperature by employing Mg-δ-doping. Furthermore, the measured Mg acceptor activation energy (E_A) was also reduced from 180 meV in uniformly Mg-doped p-type $Al_{0.07}Ga_{0.93}N$ to 160 meV in Mg-δ-doped p-type $Al_{0.07}Ga_{0.93}N$, which may be attributed to the enhanced free hole concentrations in Mg-δ-doped p-type $Al_{0.07}Ga_{0.93}N$. However, the results shown in the inset of Fig. 10(a) could also mean that the conduction mechanism is modified in Mg-δ-doped p-type layers over the uniformly doped layers. We have also carried out preliminary studies of the vertical transport properties of Mg-δ-doped p-type layers, which are more critical to the performance of UV emitters. Our preliminary results obtained on p-type GaN shown in Fig. 10(b) have shown that we could obtain a 5-fold reduction in vertical resistivity in Mg-δ-doped p-type layers compared with uniformly Mg-doped p-type layers.

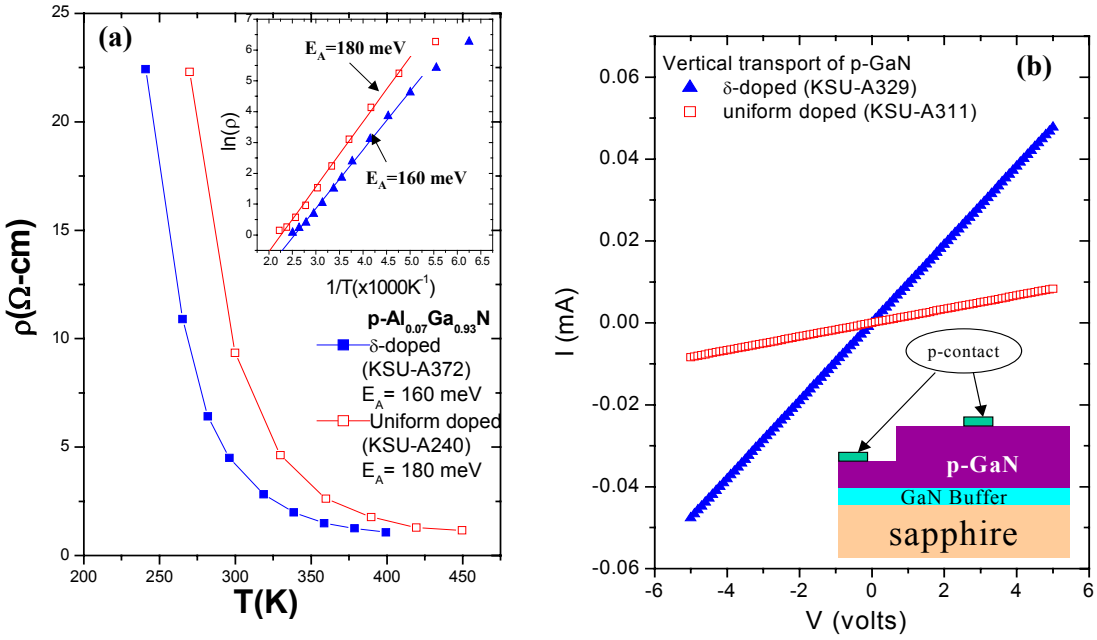

Fig. 10 (a) Resistivity (ρ) of representative uniformly Mg-doped and Mg-δ-doped p-AlGaN epilayers as functions of temperature. The inset is the Arrhenius plots of the resistivity, which indicates that δ-doping reduces the activation energy of Mg acceptors in AlGaN. (b) Comparison of "quasi" vertical transport properties of Mg uniformly doped and Mg-δ-doped p-type GaN. Etching depth (0.5 μm) and p-type Ohmic-contact geometry were nominally identical for the two samples, as accomplished by ICP etching and photolithography patterning. A 5-fold reduction in vertical resistivity was observed in Mg-δ-doped p-type layers compared with uniformly Mg-doped p-type layers.

Furthermore, comparison measurements for the PL emission spectra of Mg-δ-doped and uniformly Mg-doped GaN and AlGaN epilayers have also been carried out. The PL emission intensities associated with the band-to-impurity transition line, as well as with the exciton bound to acceptor transition line (I_1 around 3.44 eV for GaN and 3.57 eV for AlGaN), are enhanced in Mg-δ-doped layers, pointing to a reduction of non-radiative recombination centers. This corroborates the results shown in Fig. 9 – dislocation density is reduced in Mg-δ-doped epilayer layers. Thus, all of our experimental data, including electrical, optical and structural data, imply that Mg-δ-doping improves not only the p-type conduction, but also the overall quality of III-nitride films.

In addition to the reduction of dislocation density giving rise to a more efficient doping, we believe that auto-compensation of Mg impurities is also reduced in Mg-δ-doped layers. Due to the relatively large Mg ionization energy in p-type GaN of about 160 mV, only about 1% of the Mg impurities are ionized at room temperature. Therefore, high doping incorporation of Mg impurities around 10^{20} cm^{-3} is a routine practice in nitride optoelectronic and electronic device structures. Self-compensation is more likely under the condition of high Mg doping levels. During the δ-doping process, however, the Mg impurity incorporation process is modified compared with that of uniform doping. Since the Ga (and Al) atoms supply is halted, Mg impurities are more likely to replace the Ga or Al atoms during the δ-doping process. This would reduce Mg impurity self-compensation and enhance hole concentrations in Mg-δ-doped GaN and AlGaN.

It has been demonstrated recently by several groups that incorporating Mg-doped AlGaN/GaN superlattice structure into devices could enhance the hole conduction in the lateral direction. However, the enhancement of hole conduction in the vertical direction by employing superlattice structure is limited because a superlattice structure simultaneously introduces potential barriers for hole conduction in the vertical direction due to the presence of higher bandgap materials. On the contrary, δ-doping does not introduce any potential barriers in the vertical direction and is expected to enhance the vertical transport as well as the lateral transport of holes.

8. Achieving AlN epitaxial layers with high optical quality

AlN has a number of desirable characteristics for photonic applications, including a high direct bandgap of approximately 6.1 eV at room temperature, high thermal conductivity, hardness, and chemical resistance. Unlike many other III-nitride compounds, however, measuring the optical and electrical properties of AlN has been a challenge because the material is a good insulator, which renders some standard characterization methods, such as Hall measurement, useless.

We have developed a deep-UV laser spectroscopy system that allows them to make picosecond time-resolved photoluminescence measurements of AlN and, thus, to characterize and thereby improve the material's quality. The system is a frequency-quadrupled Ti:sapphire laser and provides a 3-mW and 196-nm laser emission that excites the sample. Because only high-quality semiconductor materials emit predominantly exciton photoluminescence, the spectra reveal the optical quality of the sample. We have achieved AlN epilayers with smooth surface morphology and high optical qualities that are comparable to GaN (see Figure 11).

Determining the quality of the material is key to improving the manufacturing process. Because AlN and many of its III-nitride cousins are grown on foreign substrates, defects, dislocations, and impurities are a significant problem. The new work indicates that it is possible to make AlN that displays less thermal quenching of the emission intensity and fewer problems resulting from impurities, dislocations and nonradiative recombination channels than GaN. The work has received wide interest. Figure 1 shows a new coverage by *Photonic Spectra* reporting our AlN epitaxial growth.

SEM and AFM Images of AlN

Layer structures

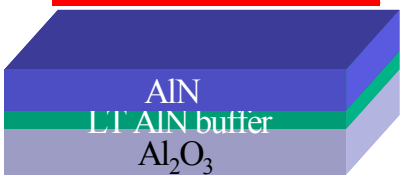

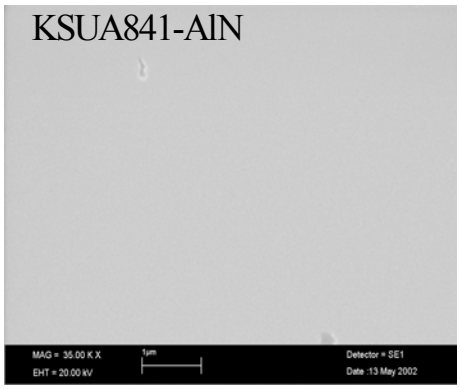

AFM RMS = 0.8 nm for 10 μm x 10 μm scan

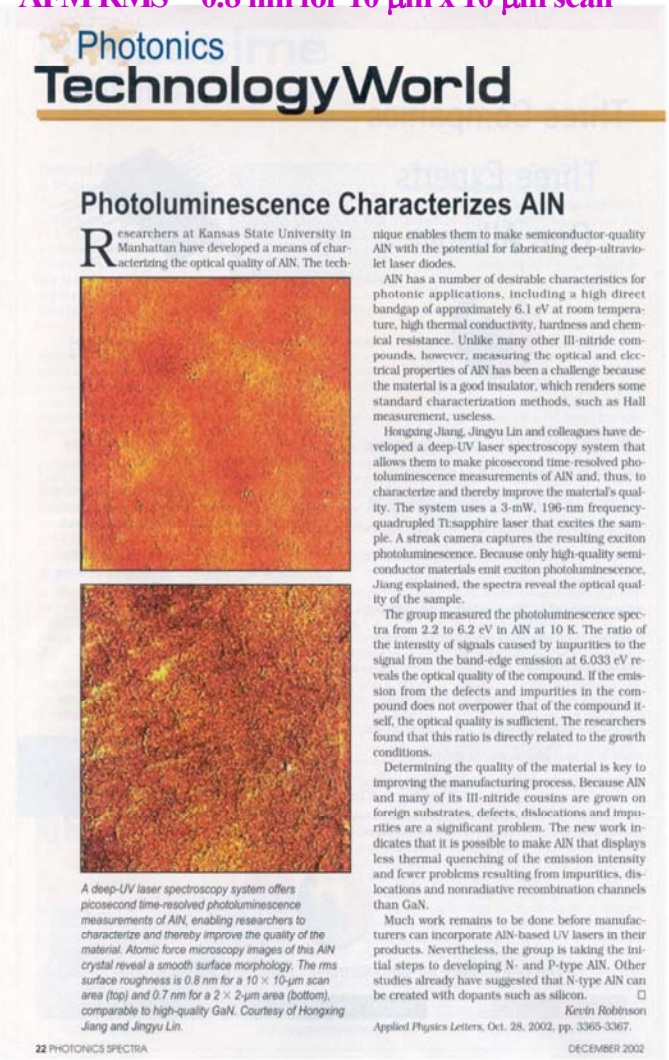

Photonics
TechnologyWorld

Photoluminescence Characterizes AlN

Researchers at Kansas State University in Manhattan have developed a means of characterizing the optical quality of AlN. The technique enables them to make semiconductor-quality AlN with the potential for fabricating deep-ultraviolet laser diodes.

AlN has a number of desirable characteristics for photonic applications, including a high direct bandgap of approximately 6.1 eV at room temperature, high thermal conductivity, hardness and chemical resistance. Unlike many other III-nitride compounds, however, measuring the optical and electrical properties of AlN has been a challenge because the material is a good insulator, which renders some standard characterization methods, such as Hall measurement, useless.

Hongxing Jiang, Jingyu Lin and colleagues have developed a deep-UV laser spectroscopy system that allows them to make picosecond time-resolved photoluminescence measurements of AlN and, thus, to characterize and thereby improve the material's quality. The system uses a 3-mW, 196-nm frequency-quadrupled Ti:sapphire laser that excites the sample. A streak camera captures the resulting exciton photoluminescence. Because only high-quality semiconductor materials emit exciton photoluminescence, Jiang explained, the spectra reveal the optical quality of the sample.

The group measured the photoluminescence spectra from 2.2 to 6.2 eV in AlN at 10 K. The ratio of the intensity of signals caused by impurities to the signal from the band-edge emission at 6.033 eV reveals the optical quality of the compound. If the emission from the defects and impurities in the compound does not overpower that of the compound itself, the optical quality is sufficient. The researchers found that this ratio is directly related to the growth conditions.

Determining the quality of the material is key to improving the manufacturing process. Because AlN and many of its III-nitride cousins are grown on foreign substrates, defects, dislocations and impurities are a significant problem. The new work indicates that it is possible to make AlN that displays less thermal quenching of the emission intensity and fewer problems resulting from impurities, dislocations and nonradiative recombination channels than GaN.

Much work remains to be done before manufacturers can incorporate AlN-based UV lasers in their products. Nevertheless, the group is taking the initial steps to developing N- and P-type AlN. Other studies already have suggested that N-type AlN can be created with dopants such as silicon. □

Kevin Robinson

Applied Physics Letters, Oct. 28, 2002, pp. 3365-3367.

A deep-UV laser spectroscopy system offers picosecond time-resolved photoluminescence measurements of AlN, enabling researchers to characterize and thereby improve the quality of the material. Atomic force microscopy images of this AlN crystal reveal a smooth surface morphology. The rms surface roughness is 0.8 nm for a 10 × 10-μm scan area (top) and 0.7 nm for a 2 × 2-μm area (bottom), comparable to high-quality GaN. Courtesy of Hongxing Jiang and Jingyu Lin.

22 PHOTONICS SPECTRA DECEMBER 2002

Fig. 11 Photoluminescence Characterizes AlN: our work on AlN epitaxial growth and PL studies was reported by Photonics Spectra (December, 2002 issue).

II. List of Publications

We have disseminated our research results through publications in scientific journals. The supporting period, we have published many papers in peer reviewed scientific journals. A partial list of our papers that have acknowledged ARO support is provided below:

1. K. C. Zeng, J. Li, J. Y. Lin, and H. X. Jiang, "Well Width Dependence of Quantum Efficiencies of GaN/$Al_xGa_{1-x}N$ Multiple Quantum Wells," Appl. Phys. Lett. 76, 3040 (2000).
2. Eun-joo Shin, J. Li, J. Y. Lin, and H. X. Jiang, "Barrier Width Dependence of Quantum Efficiencies of GaN/$Al_xGa_{1-x}N$ Multiple Quantum Wells," Appl. Phys. Lett. 77, 1170 (2000).
3. T. N. Oder, J. Li, J. Y. Lin, and H. X. Jiang, "Photoresponsivity of ultraviolet detectors based on InAlGaN quaternary," Appl. Phys. Lett. 77, 791 (2000).
4. S. X. Jin, J. Li, J. Y. Lin, and H. X. Jiang "InGaN/GaN Quantum Well Interconnected Microdisk Light Emitting Diodes," Appl. Phys. Lett. 77, 3236 (2000).
5. J. Li, K. B. Nam, K. Kim, J. Y. Lin, and H. X. Jiang "Growth and Optical Properties of InAlGaN Quaternat Alloys," Appl. Phys. Lett. 78, 61 (2000).
6. H. X. Jiang, S. X. Jin, J. Li, J. Shakya, and J. Y. Lin, "III-Nitride Blue Microdisplays," Appl. Phys. Lett. 78,1303 (2001).
7. K. B. Nam, J. Li, K. H. Kim, J. Y. Lin, and H. X. Jiang, "Growth and Deep UV Picosecond Time-Resolved Photoluminescence Studies of GaN/AlN Multiple Quantum Wells," Appl. Phys. Lett. 78, 3690 (2001).
8. S. X. Jin, J. Li, J. Shakya, J. Y. Lin, and H. X. Jiang, "Size Dependence of III-Nitride Microdisk Light Emitting Diode Characteristics," Appl. Phys. Lett. 78, 3532 (2001).
9. T.N. Oder, J.Y. Lin and H.X. Jiang, "Fabrication and Optical Characterization of III-Nitride Sub-micron Waveguides," Appl. Phys. Lett. 79, 12 (2001).
10. T.N. Oder, J.Y. Lin and H.X. Jiang, "Light Propagation properties in AlGAN/GaN Quantum Well Waveguides," Appl. Phys. Lett. 79, 2511 (2001).
11. J. Li, K. B. Nam, J. Y. Lin, and H. X. Jiang, "Optical and Electrical Properties of Al rich AlGaN Alloys," Appl. Phys. Lett. 79, 3245 (2001).
12. J. Li, T. N. Oder, M. L. Nakarmi, J. Y. Lin, and H. X. Jiang, "Optical and Electrical Properties of Mg-doped p-type AlGaN," Appl. Phys. Lett. 80, 1210 (2002).
13. K. B. Nam, J. Li, M. L. Nakarmi, J. Y. Lin, and H. X. Jiang, "Achieving highly conductive AlGaN alloys with high Al contents," Appl. Phys. Lett. 81, 1038 (2002).
14. J. Li, K. B. Nam, M. L. Nakarmi, J. Y. Lin, and H. X. Jiang, "Band-edge Photoluminescence of AlN Epilayers," Appl. Phys. Lett. 81, 3365 (2002).
15. K.B. Nam, J. Li, M. L. Nakarmi, J. Y. Lin and H. X. Jiang, "Deep ultraviolet picosecond time-resolved photoluminescence studies of AlN epilayers," Appl. Phys. Lett. 82, 1694 (2003).
16. M. L. Nakarmi, K. H. Kim, J. Li, J. Y. Lin and H. X. Jiang, "Enhanced P-type Conductions in GaN and AlGaN by Mg-Delta-Doping," App. Phys. Lett. 82, 3041 (2003).
17. T. N. Oder, J. Shakya, J. Y. Lin and H. X. Jiang "Nitride Microlens Arrays for Blue and UV Wavelength Applications, Appl. Phys. Lett. 82, 3692 (2003).
18. K. H. Kim, J. Li, S. X. Jin, J. Y. Lin, and H. X. Jiang, "III-Nitride Ultraviolet Light Emitting Diodes with Delta Doping," Appl. Phys. Lett. 83, 566 (2003).

III. Technology Transfer

The research pursued in this project is related to studies in the forefront research of III-nitride materials science and device physics. It involves novel structures using state of the art epitaxy and advanced materials and device characterization and physical property measurements. The results of these studies will have a direct impact on a number of important III-nitride technologies such as UV/blue micro-optoelectronic devices microcavity light emitting diodes, microcavity laser diodes, and vertical cavity surface emitting lasers.

Currently, we have developed a close collaboration with the Army Research Laboratory. Together, we plan to employ femtosecond as well as picosecond optical spectroscopy measurements to probe the fundamental properties of III-nitride photonic structures and devices. The results will be used to develop optimal materials and devices structures for specification applications for the Army.